NEURAL NETWORKS FOR OIL SPILL DETECTION USING ERS AND ENVISAT IMAGERY

Emanuele Angiuli, Fabio Del Frate, Luca Salvatori

Dipartimento di Informatica Sistemi e Produzione -Tor Vergata University
Via del Politecnico, 1 I-00133 Rome, Italy. Tel: +39 06 72597734, Fax +39 06 72597460
delfrate@disp.uniroma2.it

ABSTRACT

Synthetic Aperture Radar (SAR) images from satellite missions provide a significant support to oil spill detection applications. On the other hands recent studies have demonstrated the potentialities of artificial neural networks for discrimination, starting from SAR imagery, between oil spills and objects which resemble oil spills (called "look-alikes"). The oil spill detection algorithm basically consists of three steps: the identification of dark spots over the sea, the computing of a set of parameters (features) for each dark spot and the classification of the oil spill candidate using a trained neural network, where the network input is a vector containing the values of the features extracted. In this study we report the results obtained by means of a sensitivity analysis and a robustness analysis of the algorithm. This latter includes the introduction of a processability index of the images to be processed.

1. INTRODUCTION

The radar backscattering cross section from clean water surfaces at incidence angles between 25 and 60 degrees can be described by Bragg scattering theory. According to this the sea clutter is mainly due to the short gravity and the gravity–capillary waves (from one centimetre to decimetres). The presence of an oil film on the sea surface damps these kinds of waves because of the resonance-type behaviour of the viscous-elastic surface films described by the Marangoni damping theory [1], [2]. So the presence of an oil film on the sea surface drastically reduces the measured backscattering energy, resulting in darker areas in SAR imagery. However, careful interpretation is required because dark areas might also be caused by natural dark patches as natural films, grease ice, low wind speed areas (wind speed < 3 m/s), wind sheltering by land, rain cells, shear zones, internal waves, etc... To avoid false alarms experienced image interpreters or well-tuned classification algorithms are necessary. The knowledge of the local wind vector is also important because it is the responsible of the short gravity and the gravity–capillary waves, so the wind speed can strongly influence the appearance of the oil slick in a SAR image. Mostly classification algorithms for oil spill detection rely on Bayesian or other statistically-based decisions. The drawback of these methods is the complex process to develop classification rules, due to the many nonlinear and poorly understood factors involved. These kinds of difficulties can be overcome by considering a neural network approach. The use of neural networks in remote sensing has often been found effective, since they can simultaneously handle nonlinear mapping of a multidimensional input space onto the output one and cope with complex statistical behavior [3]. Neural networks, conversely, from statistically-based classifiers, do not require an explicitly well defined relationship between the input and the output vectors, as they determine their own input-output discriminant relations directly from a set of training data, used to draw the decision boundaries. In this paper, besides introducing the neural network approach, we report some results regarding its sensitivity to the considered inputs and its robustness.

2 . THE ALGHORITM FOR THE OIL SPILL DETECTION

The proposed algorithm starts with the definition of a region of interest by the user, containing an oil slick candidate (a dark spot). Analysis of the backscattering coefficient in this region is carried out and, in particular, a histogram is produced to calculate the threshold used to determine the slick contour. Subsequently, the human operator can either accept the result or reject it and produce a new edge detection by changing the threshold manually. This makes the oil spill analysis tool flexible and adaptive to a variety of situations. Once the border of the dark object is accepted, a mask is generated and a number of morphological and physical parameters are computed. In order to determine the most suitable parameters (features) to characterize the slicks, we have analysed the physical-geometrical characteristics of the dark spots, and in particular we have considered the following features, grouped for category [4], [5]:

- Analysis of the border backscattering intensity gradient:
  - *Max Gradient (GMax)*. The maximum value (in dB) of border gradient.
  - *Mean Gradient (GMe)*. The mean value of border gradient (in dB).
  - *Gradient Standard Deviation (GSd)*. The standard deviation (in dB) of the border gradient values.
- Analysis of the shape:
  - *Area (A)*. Area (in km^2) of the object.
  - *Perimeter (P)*. Length (in km) of the border of the object.

Proceedings of SEASAR 2006, 23-26 January 2006, Frascati, Italy,
(ESA SP-613, April 2006)

- *Complexity (C)*. It is defined as follows: $C = \frac{P}{2\sqrt{\pi A}}$
- *Spreading (S)*. It is derived from the principal components analysis [6] of the vectors whose components are the coordinates of the pixels belonging to the object. If λ_1 and λ_2 are the two eigenvalues associated with the computed covariance matrix and $\lambda_1 > \lambda_2$, the spreading value *S* is computed using the expression: $S = \frac{100\lambda_2}{\lambda_1 + \lambda_2}$

- Analysis of the homogeneity of the slick and of its contrast with respect to the background:
  - *Object Standard Deviation (OSd)*. The Standard deviation (in dB) of the intensity values of the pixels belonging to the oil spill candidate.
  - *Background Standard Deviation (BSd)*. The Standard deviation (in dB) of the intensity values of the pixels belonging to the region of interest, selected by the user, surrounding the object.
  - *Max Contrast (ConMax)*. The difference (in dB) between the background mean value and the lowest value inside the object.
  - *Mean Contrast (ConMe)*. The difference (in dB) between the background mean value and the object mean value.
- Analysis of the wind conditions:
  - *Wind Speed (WS)*. It is calculated by means of the inversion of the CMOD4 model [7].

The extracted features are used as inputs for a trained artificial neural network [8] which is able to classify the dark spots as oil spills or "look-alikes". In particular the local wind speed has been calculated using an inversion of the CMOD4, an empirical model used by ESA to retrieve wind vectors from ERS C-band scatterometer measurements.
The wind speed estimations have been successfully validated with the information provided by the NASA wind-scatterometer QUIKSCAT.

Starting from an archive of about 70 images mainly taken over Mediterranean basin we extracted 189 dark objects, 111 oil spills and 78 look-alikes. For a number of examples ground-truth was available, else the discrimination was based on the independent judgment of experienced image analysts. Several attempts have been initially made to properly select the number of units to be considered in the hidden layers of the neural network. The topology 12-8-8-1 has been finally chosen for its good performances both in terms of classification accuracy and of training time. For neural network simulations we used the SNNS software [9]. The evaluation of the neural net performance consists in the analysis of its behaviour once it is tested on a set of new examples, not belonging to the training set. To this purpose we divided the examples in two sets: a training set of 129 examples and a test set of 60 examples. After the training based on the learning set we found a mean square error (MSE) of 0.06621 on the test set (4 misclassified examples over a total of 60).

3 THE SENSITIVITY ANALYSIS

Starting from the available data-set, a sensitivity analysis of the features has been carried out by means of two methods: a leave-one-out procedure applied to the network inputs and an extended pruning procedure operated on the trained network. With the first method we evaluate the network classification performances in terms of rmse and of misclassification rate, removing, in turn, one of the inputs. In Table 1 the results of this analysis are summarized.

		RMS	Misclassified samples over a total of 60 samples	Δ% RMS	Δ% (misclassif. rate)
All 12 inputs		0.227	3		
11 inputs without	A	0.240	3.9	+ 5.62%	+ 30%
	P	0.229	3.2	+ 0.81%	+ 6.66%
	C	0.236	3.4	+ 3.81	+ 13.33%
	S	0.236	3.1	+ 4.1%	+ 3.33%
	Osd	0.241	4	+ 5.92%	+ 33.33%
	BSd	0.398	13	+ 75.31%	+ 433.33%
	ConMax	0.234	3.5	+ 3.11%	+ 16.66%
	ConMe	0.233	3.5	+ 2.72 %	+ 16.66%
	GMax	0.231	3.8	+ 1.77%	+ 26.66%
	GMe	0.229	3.1	+ 0.87%	+ 3.33%
	GSd	0.244	4	+ 7.47%	+ 33.33%
	WS	0.228	3.8	+ 0.24%	+ 26.66%

Table 1: Network classification performance with leave-one-out method

From this analysis we observe that discarding one input we have a general decrease of the classification accuracy in agreement with the ability of the NNs to constructively use the different pieces of information. But in most cases this worsening does not exceed the value of 10% in terms of rmse (the most significant exception is represented by BSd). In general physical features seem to be more significant than geometrical features.
The second method for sensitivity analysis was based on an extended pruning procedure which is briefly illustrated. During a pruning procedure a network is examined to assess the relative importance of its weights, and the less important ones are deleted by using the magnitude of a weight value as a measure of its importance. Typically this is followed by further training of the pruned network. By mean of this procedure it is possible simplify the topology of the neural network without worsening its performance. In the attempt to examine which features, in the chosen context, contain less information for the classification task, the pruning procedure may be prolonged to the input layer (extended pruning procedure) until 11 of the 12 components of the input vector are removed (we remind that an input or hidden unit is removed when it has lost all its connections). At the end of this analysis it is possible to label the features according to different classes of significance, deduced from the order of removal of the corresponding input units. The result of the extended pruning procedure in our case is synthetically reported in Table 2, where the features are classified through three levels of significance. This classification has been performed carrying out the pruning procedure several times over different trained networks.

Level of Significance	Features
1	BSd, GSd, OSd, WS
2	A, P, ConMax, ConMe
3	C, S, GMax, GMe

Table 2: Classification of the features significance according to their order of removal by applying the extended pruning procedure

Also from this analysis we observe that the background standard deviation belong to the first class of level of significance. This confirms the importance of this feature in the problem of oil spill detection. The local wind speed, the standard deviation of the gradient of the backscattering value at the border between the background and the oil spill and the standard deviation of the intensity values of the pixels belonging to the oil spill candidate seem to be other significant quantities according to the extended pruning analysis. Starting from this latter result, we made a test on the performance of the neural network without the less significant inputs (C, S, GMax and GMe).By retraining the neural network with only the most important 8 inputs, we have obtained results very close to those obtained considering all inputs, confirming the scarce importance of C, S, GMax and GMe on the performance on the neural network.

4 ROBUSTNESS ANALYSIS

This exercise has been made with the aim of evaluating the performance of the neural networks in presence of noisy data. To do this we firstly derived a 'Processability Index' (PI). The PI is based on the backscattering standard deviation, calculated over the whole image, of the sea surface pixels. Then we split our data set in two groups: images with a high processability index (low noise) and images with a low processability index (high noise).

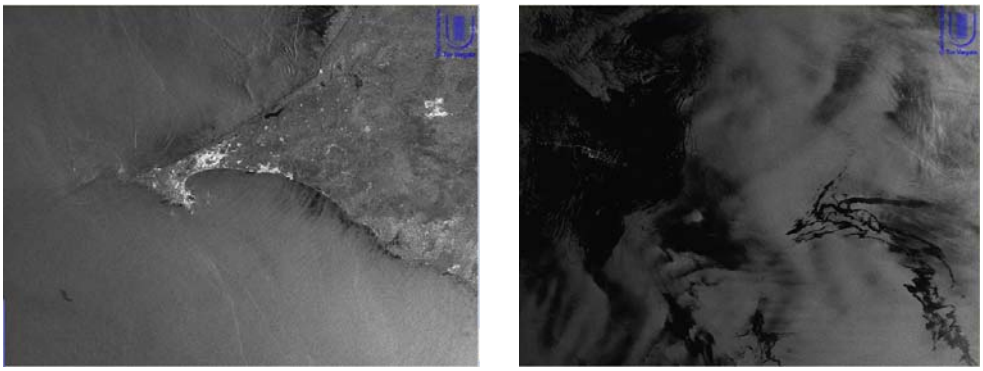

Figure 1. Images haracterized by high (left) and low (right) values of processability images.

These two groups have been used to examine the effect on the network performance using a training data set and a test data set with different levels of noise. In Fig. 2 we report the histrogram illustrating the ditribution of the extracted dark spots according to the correspondin images PI values while Table 3 summarizes the classification results obtained with this kind of analysis.

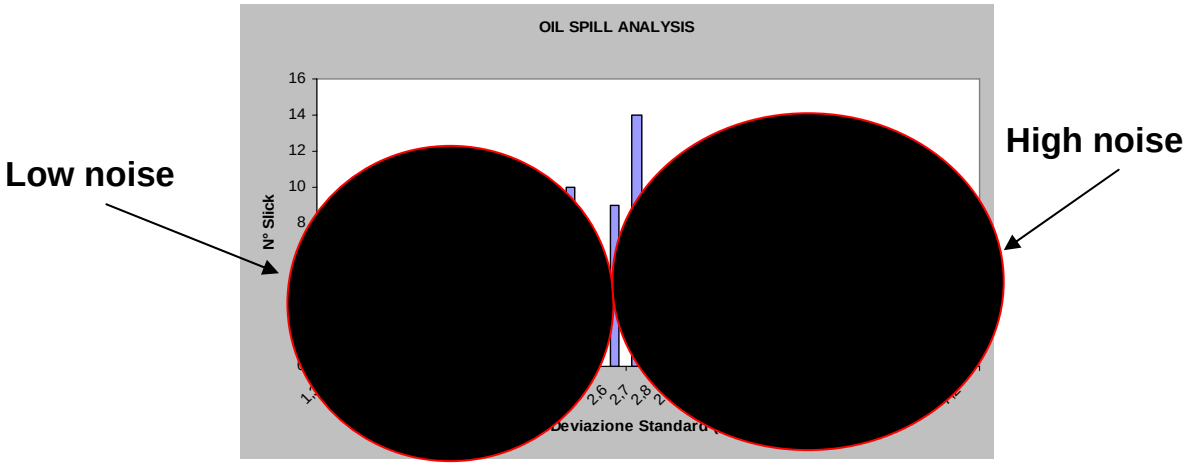

Figure 2. Distribution of the dark spots according to the PI values

Train with	Test with	Misclas. rate
Low noise data	High noise data	19%
High noise data	Low noise data	24%
All noise data	All noise data	16%

Table 3: network classification performances according to the level noise of the train and of the test set.

As expected, the best results are obtained when both training set and test set are characterized by the same level of noise, whereas the worst performance occurred when a neural network, trained with a high noisy data set, is tested with a low noisy data set. These results indicate that an adaptative approach should help in managing the problems of classification. This means that different nets for differents ranges of PI values should be designed and, in the operative mode, the suitable net should be used according to the previosly calculated noise level of the image to be processed.
A further analysis on the robustness of the oil spill algorithm has been carried out processing a preliminary set of ENVISAT ASAR images with a neural network trained with a data set composed only by ERS SAR images.

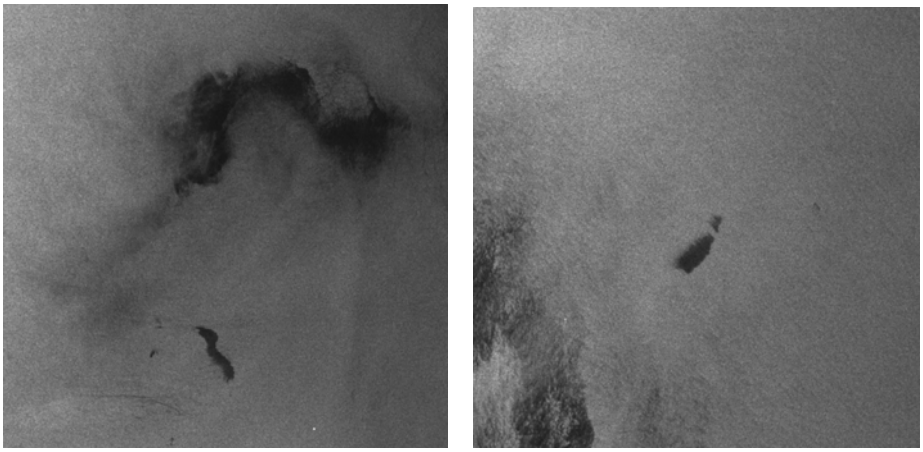

Fig. 3: Look-alikes detected by the neural algorithm on Envisat images

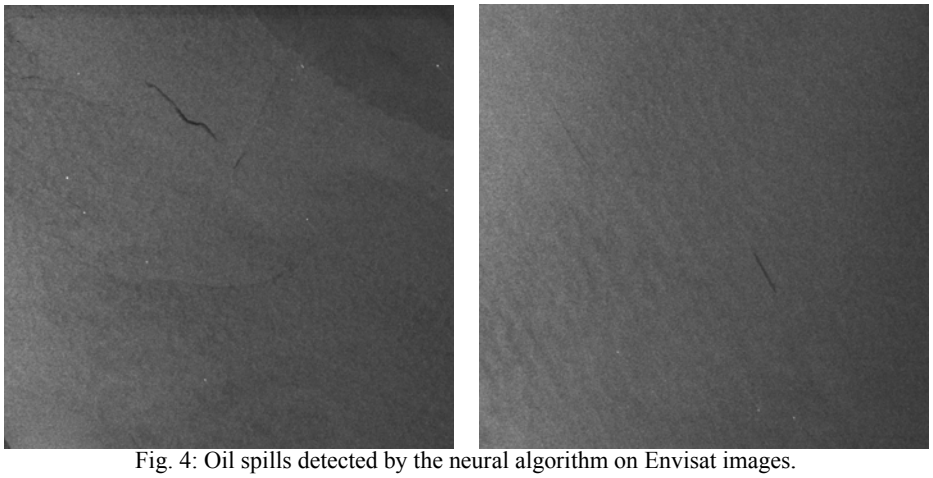

Fig. 4: Oil spills detected by the neural algorithm on Envisat images.

An overall calssification accuracy of 85% has been obtained over a limited test set of 20 examples. Even if the set used was small, these results are encouraging and seem to indicate a good robustness of the oil spills classificators, based on neural networks, when used on SAR images coming from different sensors. The robustness in this case should stem from the fact that the procedure works with radiometrically calibrated data which, focusing on the backscattering coefficient rather then on the digital number derived by simple image processing, allow better properties of generalization.

5 CONCLUSIONS

Neural network algorithms seem to be a valid alternative to Bayesian algorithms for the detection of oil spills in satellite SAR imagery. The neural network obtained after the training phase is able to correctly discriminate over a set of independent examples between oil spills and look-alikes with a largely acceptable rate of success. A sensitivity analysis pointed out which input features should be more useful for a correct classification. Even though the results obtained with such a sensitivity exercise may include some effects due to the particular considered data-set, some indications seemed very clear, for example the significance of the information content of the standard deviation of the backscattering in the background. Tests on subsets of images characterized by the same or different noise levels with respect to the one characterizing the training set have also been carried out and the obtained results suggested that an adaptive approach for the design of future neural networks dedicated to this kind of application could be more effective. Preliminary tests carried out on ENVISAT images are also encouraging, even if a more systematic validation exercise is currently ongoing. All the shown results will be exploited for the design of effective fully automatic procedures, whose development is the purpose of next activities in this field. The processing chain of the fully automatic procedure should reflect the block-diagram shown in Fig. 5.

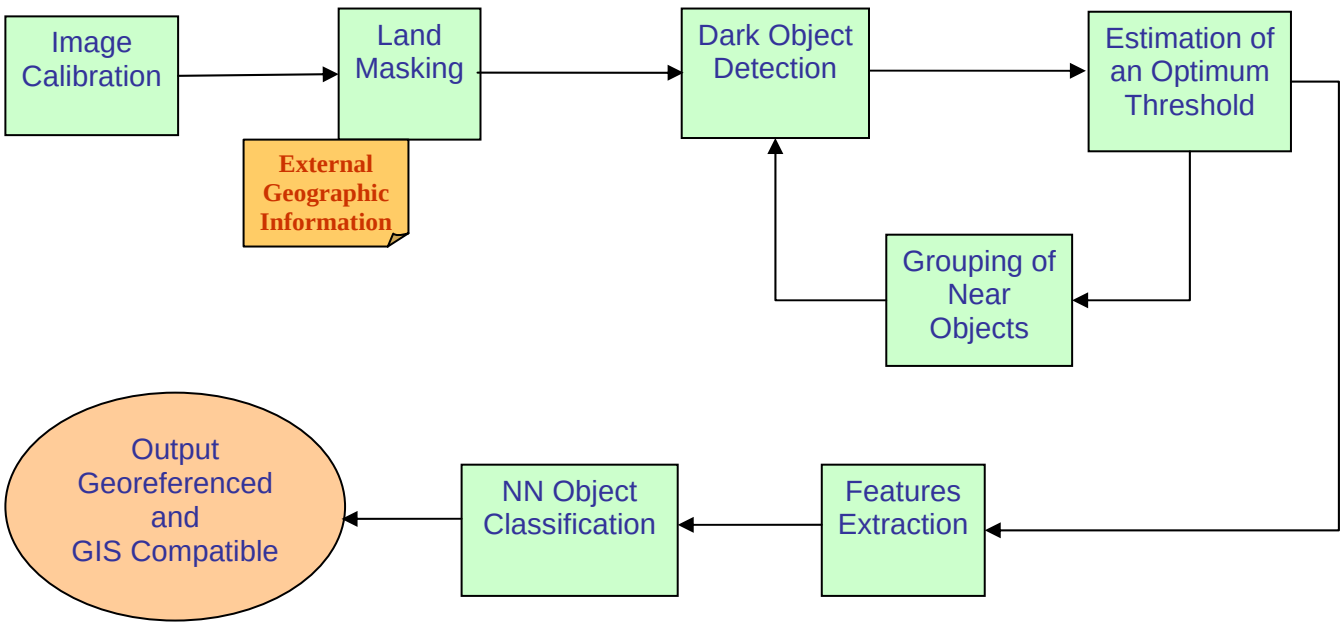

Fig. 5: Block-diagram for fully automatic oil spill detection

REFERENCES

[1] W. Alpers, and H.Huhnerfuss, "Radar signatures of oil films floating on the sea surface and the Marangoni effect", Journal of Geophysical Research, vol.93, pp.3642--3648, 1988.

[2] W. Alpers, and H.Huhnerfuss, "The damping of ocean waves by surface films: a new look at an old problem", Journal of Geophysical Research, vol.94, pp.6251--6265, 1989.

[3] Dd M. S. Dawson, "Applications of electromagnetic scattering models to parameter retrieval and classification," in *A. Fung Microwave Scatterin and Emission Models and their Application*. Norwood, MA: Artech House, 1994.

[4] F. Del Frate, A. Petrocchi, J. Lichtenegger, G. Calabresi, "Neural networks for oil spill detection using ERS-SAR data", IEEE Trans. Geoscience and Remote Sensing, Vol.38, No.5, pp. 2282—2287, 2000.

[5] F. Del Frate, L. Salvatori, J. Lichtenegger, A. Petrocchi**,** "Sea Pollution Monitoring with Neural Networks and Satellite Data", proceedings of "2003 Tyrrhenian International Workshop on Remote Sensing", pag.649-656, 2003.

[6] I.T. Jolliffe, *Principal Component Analysis*, New York: Springer-Verlag, 1986.

[7] P. Lecomte, "*CMOD4 Model Description"*, ESA-ESRIN.

[8] C. M. Bishop, "*Neural Networks for Pattern Recognition"*, Oxford Univ. Press, pp. 374--375, 1995.

[9] A. Zell, et al., "*SNNS Stuttgart Neural Network Simulator User Manual"*, Report N6/95, University of Stuttgart, Institute for Parallel and Distributed High Performance Systems, Stuttgart, Germany, 1995.